JACS
JOURNAL OF THE AMERICAN CHEMICAL SOCIETY

Subscriber access provided by American Chemical Society

Article

Polyphosphate Ions Encapsulated in Oxothiomolybdate Rings: Synthesis, Structure, and Behavior in Solution

Emmanuel Cadot, Marie-Jos Pouet, Chantal Robert-Labarre, Charlotte du Peloux, Jrme Marrot, and Francis Scheresse

J. Am. Chem. Soc., **2004**, 126 (29), 9127-9134• DOI: 10.1021/ja048746a • Publication Date (Web): 03 July 2004

Downloaded from http://pubs.acs.org on March 31, 2009

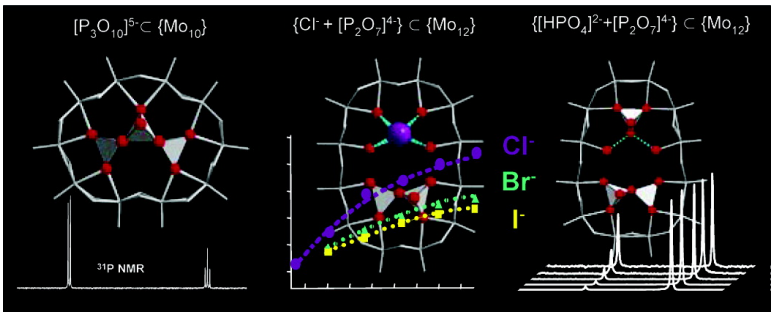

More About This Article

Additional resources and features associated with this article are available within the HTML version:

- Supporting Information
- Links to the 3 articles that cite this article, as of the time of this article download
- Access to high resolution figures
- Links to articles and content related to this article
- Copyright permission to reproduce figures and/or text from this article

View the Full Text HTML

ACS Publications
High quality. High impact.

Journal of the American Chemical Society is published by the American Chemical Society. 1155 Sixteenth Street N.W., Washington, DC 20036

J|A|C|S
ARTICLES
Published on Web 07/03/2004

Polyphosphate Ions Encapsulated in Oxothiomolybdate Rings: Synthesis, Structure, and Behavior in Solution

Emmanuel Cadot,*,† Marie-José Pouet,‡ Chantal Robert-Labarre,‡ Charlotte du Peloux,† Jérôme Marrot,† and Francis Sécheresse†

Contribution from the Institut Lavoisier, IREM, UMR CNRS 8637, Université de Versailles Saint Quentin, 45 Avenue des Etats-Unis, 78035 Versailles, France, and SIRCOB, UMR CNRS 8086, Université de Versailles Saint Quentin, 45 Avenue des Etats-Unis, 78035 Versailles, France

Received March 4, 2004; E-mail: cadot@chimie.uvsq.fr

Abstract: Cyclic oxothiomolybdates containing polyphosphate ions were prepared by simple reactions in aqueous medium of the corresponding polyphosphate ions and the cyclic precursor $K_2I_2Mo_{10}S_{10}O_{10}(OH)_{10}(OH_2)_5 \cdot 15H_2O$. $K_5[Cl(P_2O_7\}Mo_{12}S_{12}O_{12}(OH)_{12}(H_2O)_4] \cdot 22H_2O$ (**1**) was isolated from concentrated chloride solution (2.5 mol·L^{-1}). **1** reveals a remarkable complex containing two different substrates encapsulated in a dodecanuclear ring, a H-bonded Cl^- ion, and a covalently bonded $\{P_2O_7\}$ group. The chloride ion in **1** can be selectively removed for a monohydrogenophosphate group yielding $K_6[(HPO_4)(P_2O_7)Mo_{12}S_{12}O_{12}(OH)_{12}(H_2O)_2] \cdot 19H_2O$ (**2**), a mixed species containing a $\{P_2O_7\}$ and a $\{HPO_4\}$ group. The substitution is accompanied by a significant change of the ring, which adopts a "pear-shape" conformation. In the presence of triphosphate ion, the "heart-shaped" decanuclear ring $Rb_3[(H_2P_3O_{10})Mo_{10}S_{10}O_{10}(OH)_{10}] \cdot 17.5H_2O$ (**3**) is formed containing a linear $\{P_3O_{10}\}$ group intimately embedded in the inorganic cyclic host. The three compounds were structurally characterized by single-crystal X-ray diffraction. The behaviors of **1**, **2**, and **3** in solution were studied by ^{31}P NMR. Variable temperature experiments, supported by a two-dimensional COSY ^{31}P experiment, revealed that the supramolecular interaction existing between the chloride ion and the ring in solid **1** is maintained in solution. Nevertheless, **1** remains labile, and successive equilibria were evidenced and interpreted as an ion-pair association involving a halide ion (Cl, Br, or I), responsible for the conformational change of the $\{P_2O_7\}$ group within the cavity. The influence of the nature of the halide guest (Cl^-, Br^-, and I^-) on the successive equilibria was studied, and the thermodynamic constant related to the postulated equilibrium was determined. The stability of the supramolecular association decreases in the order Cl > Br > I. In solution, a phosphate exchange is observed for **2** while for **3** the absence of temperature dependence of the ^{31}P NMR spectrum confirms the conformation of the host−guest system is blocked. Elemental analysis and infrared characterizations are also supplied.

Introduction

The synthesis of designed inorganic materials of specific size, conformation, and properties is a key aspect in fields as various as modern materials, electronic, catalysis, or medicine.[1−3] There is wide structural diversity in polyoxometalate complexes, ranging from discrete clusters to extended frameworks often obtained by the directed linking of simple polyhedra or more sophisticated polyoxometalate subunits.[4] Examples have also been reported for polyoxovanadates where discrete metal oxide shells encapsulate various anionic guests.[5−7] The structural flexibility of such materials is attributed to the versatility of the coordination of vanadium centers, which can change between octahedral $\{VO_6\}$ and square pyramidal $\{VO_5\}$: the cluster shell was considered as a kind of "molecular flask" weakly interacting with the inner guest.[8] Some of these cyclic clusters derive from linear cores containing edge-shared polyhedra, and this is the case of $\{V_8O_{24}\}$.[9,10] The cyclic oxothiomolybdates that we report here exhibit some structural analogy with polyvanadates. The inorganic cyclic host of general formula $[Mo_{2n}S_{2n}O_{2n}(OH)_{2n}]$ is based on successive enchainments of $\{Mo_2O_2S_2\}$ building blocks, and the shape and size of these architectures are intimately related to the nature of the template or structure-directing agent.[11] The first member of the series is the neutral dodecanuclear ring $[Mo_{12}S_{12}O_{12}(OH)_{12}(H_2O)_6]$,[12] which delimits

† Institut Lavoisier, IREM, UMR CNRS.
‡ SIRCOB, UMR CNRS.

(1) Fujita, M.; Umemoto, K.; Yoshizawa, M.; Fujita, N.; Kusukawa, T.; Biradha, K. *Chem. Commun.* **2001**, 509−518.
(2) Yaghi, O. M.; O'Keeffe, M.; Ockwig, N. W.; Chae, H. K.; Eddaoudi, M.; Kim, J. *Nature* **2003**, *143*, 705−714.
(3) Cotton, F. A.; Donahue, J. P.; Murillo, C. A. *J. Am. Chem. Soc.* **2003**, *125*, 5436.
(4) (a) See, for example, the special issues on polyoxometalates of *Chem. Rev.* **1998**, *98* and *C. R. Acad. Sci., Ser. IIc: Chim.* **1998**. (b) *Polyoxometalates: From Platonic Solids to Anti-Retroviral Activity*; Pope, M. T., Müller, A., Eds.; Kluwer: Dordrecht, The Netherlands, 1994.
(5) Müller, A.; Krickmeyer, E.; Penk, M.; Rohlfing, R.; Armatage, A.; Bögge, H. *Angew. Chem., Int. Ed. Engl.* **1991**, *30*, 1674.
(6) Müller, A.; Reuter, H.; Dillinger, S. *Angew. Chem., Int. Ed. Engl.* **1995**, *34*, 2311.
(7) Müller, A.; Rolhfing, R.; Döring, J.; Penk, M. *Angew. Chem., Int. Ed. Engl.* **1991**, *30*, 588.
(8) Müller, A. *Nature* **1991**, *352*, 115.
(9) Huan, G.; Greaney, M. A.; Jacobson, A. J. *J. Chem. Soc., Chem. Commun.* **1991**, 260.
(10) Khan, M. I.; Chen, Q.; Zubieta, J. *Inorg. Chim. Acta* **1993**, *212*, 199.
(11) Cadot, E.; Sécheresse, F. *Chem. Commun.* **2002**, 2189.

Table 1. Summary of Crystal Structure Data

	1	2	3
formula	$K_5ClH_{64}P_2Mo_{12}O_{57}S_{12}$	$K_6H_{63}P_3Mo_{12}O_{60}S_{12}$	$Rb_3H_{47}Mo_{10}P_3S_{10}O_{47.50}$
M, g·mol^{-1}	2805.40	2887.01	2436.70
T, K	296(2)	296(2)	296(2)
cryst size (mm^3)	0.18 × 0.08 × 0.06	0.25 × 0.25 × 0.15	0.24 × 0.24 × 0.14
cryst syst	monoclinic	orthorhombic	hexagonal
space group	$P2_1/c$	$Cmc2_1$	$P6_3/m$
a, Å	9.3478(2)	11.1863(2)	23.2344(2)
b, Å	15.9535(2)	26.3305(3)	23.2344(2)
c, Å	24.4659(4)	29.6214(3)	20.7222(3)
β, deg	92.410(1)	90	90
V, Å^3	3645.4(1)	8724.7(2)	9687.9(2)
Z	2	4	6
ρ_{calcd}, g·cm^{-3}	2.556	2.198	2.506
μ (Mo Kα), cm^{-1}	2.799	2.380	4.609
λ (Mo Kα), Å	0.71073	0.71073	0.71073
θ range, deg	1.52−29.60	1.37−29.94	1.01−23.29
data collected	24423	30644	44803
unique data	9304	11617	4814
unique data $I>2\sigma(I)$	6062	10163	3747
no. params	506	551	440
$R(F)^a$	0.0503	0.0465	0.0390
$R_w(F^2)^b$	0.1082	0.1269	0.1092
GOF	1.040	1.078	1.155

$^a R_1 \frac{\sum|F_o| - |F_c|}{\sum|F_c|}$. $^b R_w = \sqrt{\frac{\sum w(F_o^2 - F_c^2)^2}{\sum w(F_o^2)^2}}$. $^c \frac{1}{w} = \sigma^2 F_o^2 + (aP)^2 + bP$.

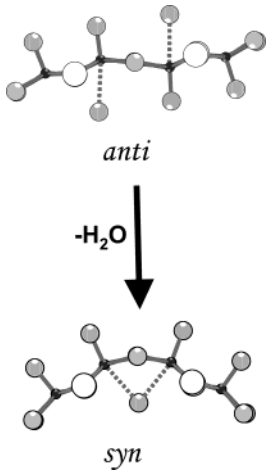

Figure 1. Anti- and syn-linkages between two $\{Mo_2O_2S_2\}$ dimers.

a central open cavity of about 11 Å in diameter, lined by six water molecules playing a crucial role in the condensation process, formally deriving from olation reactions of the hexa-aquo dication $[Mo_2O_2S_2(OH_2)_6]^{2+}$.[13] Those water molecules can be viewed as structure-directing agents, favoring the syn connection between the $\{Mo_2O_2S_2\}$ units. In the wheel, the aquo ligands attached to two neighboring $\{Mo_2O_2S_2\}$ units ensure the face-shared connections between dimers and stabilize the syn conformation represented in Figure 1, at the origin of the circular geometry. A syn/anti statistic mode of connections would have favored polymeric enchainments. In addition, these inner water molecules are polarized enough to interact smoothly through hydrogen bonds with soft bases such as halide ions.[14] The resulting supramolecular associations observed in the solid state are probably maintained in solution, explaining the solubility of neutral cyclic species. These inner water molecules can be successively ionized into hydroxo groups, giving the cyclic architecture a polyacid behavior.[15] Furthermore, these water molecules are labile enough to enhance the cationic character of the open cavity. Bases, as (poly)carboxylate, monophosphate, and metalate ions, have been substituted to the aquo ligands leading to specific host−guest compounds.[16−18] In addition, the lability of the aquo ligands, supported by the versatile geometry of the Mo(V) centers, easily swinging from octahedral to square pyramidal, confers an extreme flexibility to the ring which adapts its geometry (circular or elliptical conformation) to that of the central guests.[19,20] These properties enable to develop some challenging *molecular engineering* concepts toward recognition, dynamic, reversible inclusion of guest, and molecular adaptability.

Results and Discussion

Structures of the Anions. Crystal data are given in Table 1. The three $[Cl(P_2O_7)Mo_{12}S_{12}O_{12}(OH)_{12}(OH_2)_4]^{4-}$ (**1**) (noted $[Cl(P_2)Mo_{12}]^{4-}$), $[(HPO_4)(P_2O_7)Mo_{12}S_{12}O_{12}(OH)_{12}(OH_2)_2]^{6-}$ (**2**) (noted $[HP(P_2)Mo_{12}]^{6-}$), and $[(H_2P_3O_{10})Mo_{10}S_{10}O_{10}(OH)_{10}]^{3-}$ (**3**) (noted $[(H_2P_3)Mo_{10}]^{3-}$) molecular architectures are described as an inorganic cyclic neutral skeleton $\{Mo_{2n}S_{2n}O_{2n}(OH)_{2n}\}$, $n = 5$ or 6, encapsulating mono, di, or triphosphate guests. The "Mo-wheel" results from $[Mo_2S_2O_2]^{2+}$ building blocks linked to each others by double hydroxo bridges. Two types of Mo−Mo distances are observed: short Mo−Mo distances (ca 2.8 Å) within the binuclear unit, characteristic of a metal−metal

(12) Cadot, E.; Salignac, B.; Halut, S.; Sécheresse, F. *Angew. Chem.* **1998**, *110*, 631−633.
(13) Jolivet, J. P. *Metal Oxide Chemistry and Synthesis. From Solution to Solid State*; Wiley: Chichester, U.K., 2000.
(14) Cadot, E.; Salignac, B.; Marrot, J.; Dolbecq, A.; Sécheresse, F. *Chem. Commun.* **2000**, 261−262.
(15) Cadot, E.; Dolbecq, A.; Salignac, B.; Sécheresse, F. *J. Phys. Chem. Solids* **2001**, *62*, 1533−1543.
(16) Salignac, B.; Riedel, S.; Dolbecq, A.; Sécheresse, F.; Cadot, E. *J. Am. Chem. Soc.* **2000**, *122*, 10381.
(17) Cadot, E.; Salignac, B.; Loiseau, T.; Dolbecq, A.; Sécheresse, F. *Chem.−Eur. J.* **1999**, *5*, 3390.
(18) Dolbecq, A.; Cadot, E.; Sécheresse, F. *Chem. Commun.* **1998**, 2293.
(19) Cadot, E.; Marrot, J.; Sécheresse, F. *Angew. Chem.* **2001**, *40*, 774.
(20) Cadot, E.; Salignac, B.; Marrot, J.; Sécheresse, F. *Inorg. Chim. Acta* **2003**, *350*, 414.

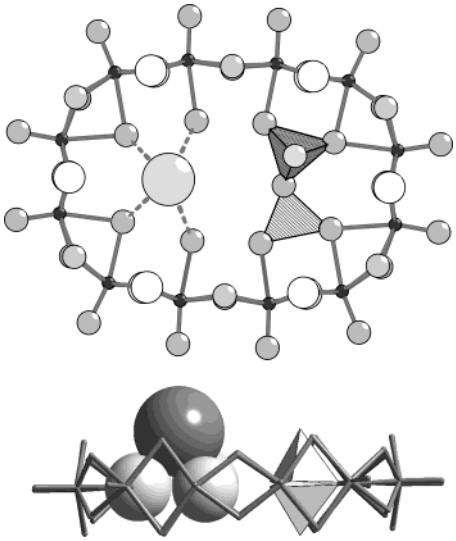

Figure 2. Top: Face view of $[Cl(P_2O_7)Mo_{12}S_{12}O_{12}(OH)_{12}(OH_2)_4]^{5-}$ (**1**). Bottom: Side view of $[Cl(P_2O_7)Mo_{12}S_{12}O_{12}(OH)_2(OH_2)_4]^{5-}$ (**1**), showing the quasi-close compact arrangement of the off-centered supramolecular cluster $\{Cl(OH_2)_4\}^-$.

bond, and long Mo−Mo interblock distances (ca 3.2 Å). The important feature of these structures is the possibility of matching their nuclearity and conformation to the shape of the guest(s). The inner phosphate ions and aquo ligands adopt different modes of coordination, singly or doubly bonded through oxygen atoms. This mode of linking provokes large variations in the Mo−Mo−Mo angles, ranging from 135° to 180°, and determines the interblock connections, either face- or edge-sharing.

$K_5[Cl(P_2O_7)Mo_{12}S_{12}O_{12}(OH)_{12}(H_2O)_4]\cdot 22H_2O$ (1). The molecular unit of **1** (Figure 2) is formed of a dodecameric cyclic backbone $\{Mo_{12}S_{12}O_{12}(OH)_{12}\}$ resulting from the self-linking of six $\{Mo_2O_2S_2\}$ fragments. A pyrophosphate $[P_2O_7]^{4-}$ ion is strongly attached in the hemicycle through four anchoring points. Two oxygen atoms of the pyrophosphate ion bridge two adjacent Mo atoms, while the other two show monodentate coordination. Finally, six Mo atoms are involved in bonding contacts with the off-centered pyrophosphate. Four water molecules attached to other six Mo atoms line the second part of the cavity. The presence of a single chloride ion on the aperture of the cavity is a striking feature of the molecular structure. The distances between the capping Cl^- ion and the oxygen atoms of the four inner aquo ligands [about 3.27(1)Å] are short enough to suggest that the stability of the supramolecular arrangement is directly related to the presence of four hydrogen bonds. As depicted in Figure 2 (bottom), the $\{Cl(OH_2)_4\}^-$ cluster exhibits a quasi-close compact arrangement. The two $\{PO_4\}$ functions of the pyrophosphate group adopt an anti conformation, with the two {P═O} bonds of each phosphate group pointing toward opposite directions. The two phosphorus atoms are slightly displaced about 0.5 Å from the mean plane defined by the 12 molybdenum atoms. The presence of the single capping chloride ion brakes any symmetry, making the two phosphate groups strictly nonequivalent in the solid state.

$K_6[(HPO_4)(P_2O_7)Mo_{12}S_{12}O_{12}(OH)_{12}(H_2O)_2]\cdot 23H_2O$ (2). The inorganic ring in **2** represented in Figure 3 derives from that of anion in **1**. The off-centered $[P_2O_7]^{4-}$ group is still present in the cavity delimited by the dodecameric ring, but the chloride

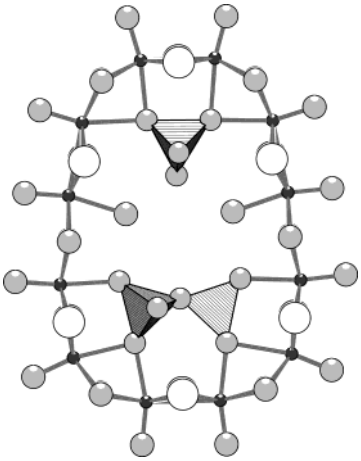

Figure 3. Representation of the mixed complex $[(HPO_4)(P_2O_7)Mo_{12}S_{12}O_{12}(OH)_{12}(OH_2)_2]^{6-}$ (**2**).

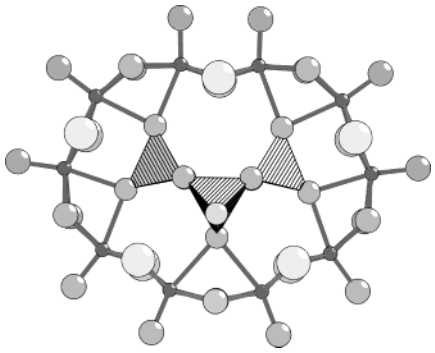

Figure 4. Representation of the "heart-shape" complex $[(H_2P_3O_{10})Mo_{10}S_{10}O_{10}(OH)_{10}]^{3-}$ (**3**).

ion and two water molecules are replaced by a monohydrogenophosphate $[HPO_4]^{2-}$ ion. The chelating phosphato group acts as a pincer, slightly distorting the wheel from regular elliptical (D_{2h} local symmetry for the Mo_{12} skeleton in **1**) to a "pear-shape" conformation in **2** (C_{2v} local symmetry). A nonprotonated {P═O} bond is identified by the significant short P−O distances [∼1.52(1) Å], while the other corresponding distance is longer enough to be attributed to a P−OH bond [∼1.59(1) Å]. In addition, the {P═O} fragment interacts weakly through hydrogen bonds with the two closest symmetrically distributed aquo ligands (O···O averaged distances of about 2.56(1) Å). Finally, this compound is the first example reporting the encapsulation of two different substrates, a monophosphate group and a pyrophosphate group, in the pocket of the $\{Mo_{12}\}$ wheel.

$Rb_3[(H_2P_3O_{10})Mo_{10}S_{10}O_{10}(OH)_{10}]\cdot 17.5H_2O$ (3). The molecular structure of **3** represented in Figure 4 corresponds to a perfect example of encapsulation of a substrate: the linear triphosphate ion $[P_3O_{10}]^{5-}$ is embedded in the pocket of the neutral Mo_{10} ring. All the Mo centers are engaged in bonding contacts with the central guest. The five oxygen atoms interacting with the host bridge the adjacent Mo atoms, yielding a host−guest anion, which adopts a "heart-shape" conformation. Elemental analysis is consistent with two fewer rubidium cations. The charge balance should be ensured by the presence of two protons, probably located on the terminal oxygen atoms of the central triphosphate, although the three corresponding experimental distances do not univocally permit their location [1.533−1.476 Å].

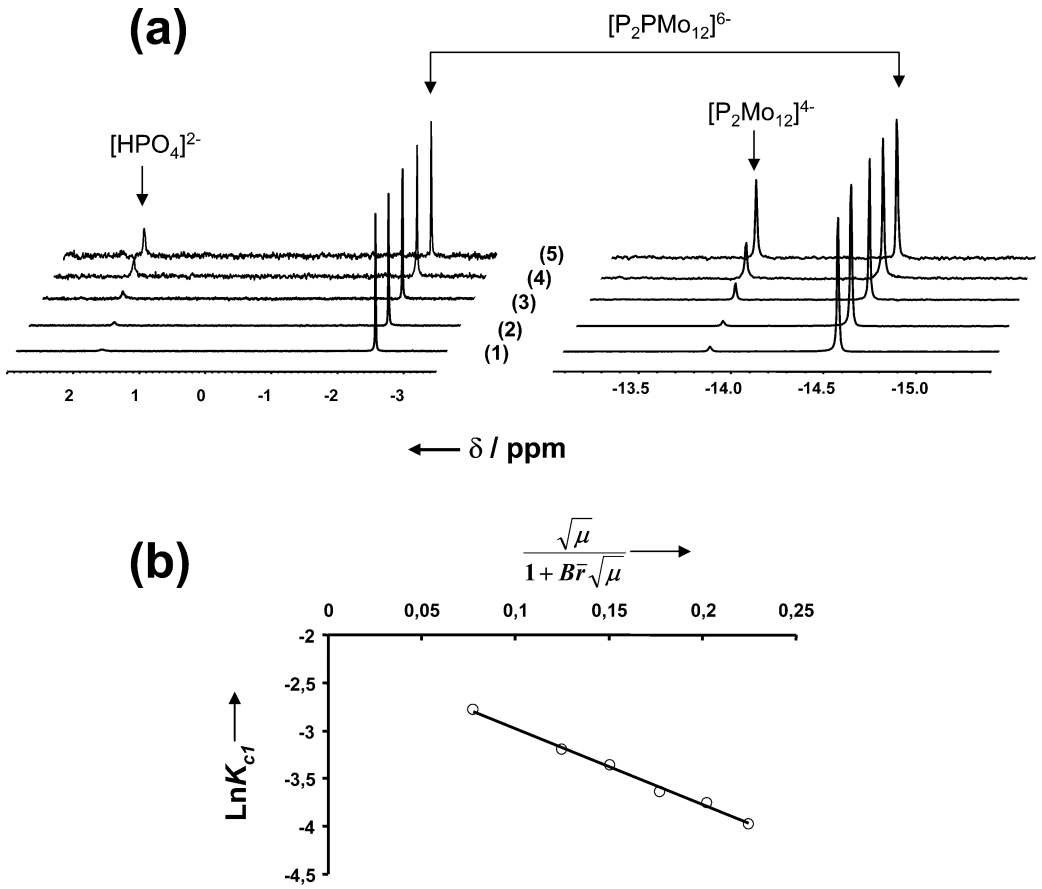

Figure 5. (a) ^{31}P NMR spectra of **2** at variable concentration: (1) 3.66×10^{-2} mol·L, (2) 1.85×10^{-2} mol·L, (3) 9.27×10^{-3} mol·L, (4) 2.54×10^{-3} mol·L; (5) 7.2×10^{-4} mol·L. (b) Linear behavior agreeing with eq 4:

$$\mathrm{LogK_{C1}} = \mathrm{LogK_1} - 16A\frac{\sqrt{\mu}}{1 + B\bar{r}\sqrt{\mu}}$$

.

^{31}P NMR Characterization of 1, 2, and 3 in Aqueous Solution $[(HPO_4)(P_2O_7)Mo_{12}S_{12}O_{12}(OH)_{12}(H_2O)_2]^{6-}$ (2). Selected ^{31}P NMR spectra of **2** recorded at room temperature are shown in Figure 5a. At high concentration (0.036 mol·L^{-1}), the spectrum exhibits only two lines with 2:1 intensity ratio consistent with a pyrophosphate ($\delta = -14.55$ ppm; 2P) and a monohydrogenophosphate ($\delta = -2.55$ ppm; 1P) encapsulated group. When the concentration is decreased from 0.04 mol·L^{-1} to 0.0007 mol·L^{-1}, two additional resonances appeared at +1.80 ppm and −13.90 ppm with an intensity ratio of about 1:2. On the basis of its chemical shifts, the +1.80 ppm line is attributed to uncoordinated phosphate $[HPO_4]^{2-}$. The remaining peak at −13.90 ppm corresponds to the $[(P_2O_7)Mo_{12}O_{12}S_{12}(OH)_{12}(H_2O)_4]^{4-}$ anion (noted $[(P_2)Mo_{12}]^{4-}$) resulting from the loss of the inner phosphate (see below). Finally, a simple preponderant equation (1) can be expressed, involving the $[HPO_4]^{2-}$ ion exchange within the cavity of the Mo_{12} ring.

$$[\mathrm{HP(P_2)Mo_{12}}]^{6-} \rightleftharpoons [\mathrm{HP}]^{2-} + [(\mathrm{P_2})\mathrm{Mo_{12}}]^{4-} \qquad (1)$$

The lability of such a group was previously observed on phosphate-containing rings and corresponds to a common feature in such systems.[17,20] In agreement with the proposed eq 1, the addition of phosphate ions to a solution of **2** prevents the formation of the $[(P_2)Mo_{12}]^{4-}$ anion. The quantitative treatment of the dilution experiments shown in Figure 5b allowed us to determine the constant K_1 of eq 1, expressed by eq 2.

$$K_1 = \frac{a_{[\mathrm{P_2Mo_{12}}]^{4-}}\, a_{[\mathrm{HP}]^{2-}}}{a_{[\mathrm{HPP_2Mo_{12}}]^{6-}}} \qquad (2)$$

Therefore, the extraction of the K_1 value required a Debye−Hückel correction since the ionic strength varies from 0.01 to 0.75. For ionic strengths $\mu > 10^{-2}$, the activity coefficient γ_i for an ion i is expressed by the extended Debye−Hückel law (eq 3)

$$\mathrm{Log}_{10}\,\gamma_i = -\frac{z_i^2 \cdot A\sqrt{\mu}}{1 + Br_i\sqrt{\mu}} \qquad (3)$$

where A and B are two defined constants (at 25 °C, in water $A = 0.509$ mol$^{-1/2}$·dm$^{3/2}$ and $B = 0.347$ mol$^{-1/2}$·dm$^{1/2}$),[21] Z_i is the ionic charge of i, and r_i is a fitting parameter corresponding to the hard-sphere collision distance for a given i ion. Generally, the r_i parameter matches approximately to the hydrodynamic

(21) Alberty, R. A.; Sylbey, R. J. *Physical Chemistry*, 2nd ed.; Wiley: New York, 1997.

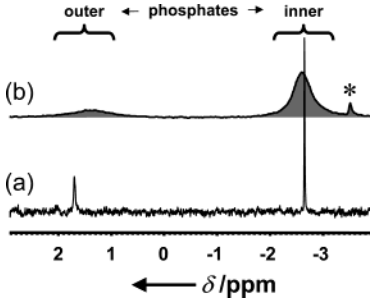

Figure 6. Monophosphate region of the ^{31}P NMR spectrum at 298 K (a) for $[(HPO_4)_2Mo_{12}S_{12}O_{12}(OH)_{12}(OH_2)_2]^{4-}$ and (b) for $[(HPO_4)(P_2O_7)Mo_{12}S_{12}O_{12}(OH)_{12}(OH_2)_2]^{6-}$.

radius of the ion. Equation 4 was obtained from eqs 2 and 3.

$$Log_{10}\,K_{c1} = Log_{10}\,K_1 - \frac{16{\cdot}A\sqrt{\mu}}{1 + B\bar{r}\sqrt{\mu}} \qquad (4)$$

In eq 4, K_{c1} is the conditional constant of eq 1 expressed with the concentration of the $[HP]^{2-}$, $[(P_2)Mo_{12}]^{4-}$, and $[HP(P_2)Mo_{12}]^{6-}$ species, and $\bar{r}$ is an adjustable parameter (averaged values of the individual r_i parameters). The best fit (see Figure 5b) was obtained with the current value of the B constant (0.347×10^{-10} $mol^{-1/2}{\cdot}dm^{1/2}$), and $\bar{r} = 10^{-8}$ dm, consistent with the dimensions of the Mo_{12} rings (about 14 Å in diameter in the solid state). The linear plot (Figure 5b) gives $K_1 = 0.0072$ and $A = 0.500$ $mol^{-1/2}{\cdot}L^{1/2}$. The low value of K_1 gives a standard Gibb's energy at 25 °C, $\Delta_r G° = 12.2$ kJ·mol^{-1}, which illustrates the high affinity of the ring for the $[HPO_4]^{2-}$ phosphate ion. Another point needing to be discussed concerns the ^{31}P line broadening of exchangeable phosphate ions in other oxothiomolybdate rings. The phosphate exchange properties in the mono and diphosphato compounds, $[(HPO_4)Mo_{10}S_{10}O_{10}(OH)_{10}(OH_2)_3]^{2-}$ and $[(HPO_4)_2Mo_{12}S_{12}O_{12}(OH)_{12}(OH_2)_2]^{4-}$, noted $[HPMo_{10}]^{2-}$ and $[(HP)_2Mo_{12}]^{4-}$, respectively, were previously reported.[17] Both compounds are related by an equilibrium involving uncoordinated phosphate ions in solution. An exhaustive study revealed the existence of dynamic exchanges involving the phosphate ions within the two compounds. At 298 K, the ^{31}P resonances of $[(HP)_2Mo_{12}]^{4-}$ and $[HPMo_{10}]^{2-}$ collapse, giving a broad signal $\Delta\nu_{1/2} = 45$ Hz (at $\delta = -2.4$ ppm) while simultaneously the line width related to the uncoordinated phosphate reaches $\Delta\nu_{1/2} = 120$ Hz. In the same conditions at 298 K for solutions of $[HP(P_2)Mo_{12}]^{4-}$, the line widths of coordinated and uncoordinated phosphates do not exceed 3 Hz. The ^{31}P NMR spectra of the monophosphate region for both the systems at 298 K are shown in Figure 6. These results suggest that the phosphate ion dynamic exchange is substantially lowered for the pyrophosphate containing Mo_{12} ring. The dynamic properties of such molecular materials are related to the extreme flexibility of the Mo_{2n} architecture and to the internal mobility of the substrate as previously reported for the Mo_{10} and Mo_{12} rings containing linear dicarboxylate ions with long alkyl chain ($[H_6C_5O_4]^{2-}$ and $[H_{10}C_7O_4]^{2-}$, respectively).[16] For such systems, ^{1}H NMR studies showed that at ambient temperature, a synergistic host−guest dynamic occurs, the wheeling of the template inside the cavity being facilitated by the flexibility of the ring. With monophosphate groups, similar internal motions must be considered, probably facilitated by the flexibility of the inorganic backbone. The line width of the $\{P_2O_7\}$ resonance is sharp (~2 Hz) and

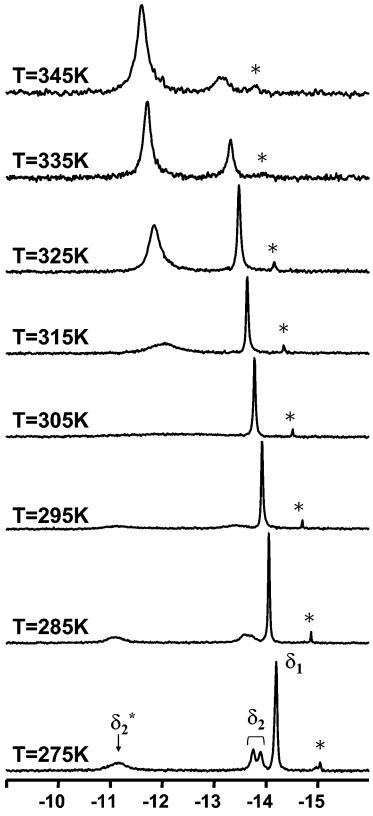

Figure 7. Variable temperature ^{31}P NMR spectra of $[Cl(P_2O_7)Mo_{12}S_{12}O_{12}(OH)_{12}(OH_2)_4]^{5-}$.

does not vary significantly with temperature, indicating that no efficient dynamic occurs on the NMR time scale. Thus, the $\{P_2O_7\}$ moiety within the Mo_{12} ring acts as a *pseudo*-pillar strongly attached to six anchoring points conferring rigidity to the hemicycle of the "pear-shape" ring. It also sterically prevents any internal hopping for the neighboring monophosphate ion.

$[Cl(P_2O_7)Mo_{12}S_{12}O_{12}(OH)_{12}(H_2O)_4]^{5-}$ (1). The variable temperature ^{31}P NMR spectra of $[ClP_2Mo_{12}]^{5-}$ in aqueous solution are shown Figure 7. At 275 K, the spectrum of **1** exhibits a sharp resonance ($\Delta\nu_{1/2} = 4$ Hz) at −14.25 ppm, noted δ_1; an asymmetric doublet at −13.85 and −13.75 ppm, noted δ_2; and a broad asymmetric line($\Delta\nu_{1/2} = 80$ Hz) at −11.15 ppm, noted δ_2*. Two additional minor lines at −14.60 and −2.60 ppm are always present in the spectra of **1** and were assigned unambiguously to the mixed $[HP(P_2)Mo_{12}]^{6-}$ compound (**2**) (see above). The formation of this compound results from the hydrolysis of the pyrophosphate group into monophosphate ions, which invariably leads to the mixed $[HP(P_2)Mo_{12}]^{6-}$ species. The spectrum of **1** is strongly temperature-dependent. The doublet, centered on $\delta_2 = -13.80$ ppm, collapses on raising the temperature just 10 K and then completely vanishes at 305 K. Similarly, the $\delta_2* = -11.15$ ppm broad line exhibits a comparable feature. Both the lines (initial doublet at −13.80 ppm and −11.15 ppm line) broaden and then mutually coalesce at 305 K, for a broad resonance at −12.00 ppm, which sharpens as the temperature increases until 345 K. The high and low temperature ^{31}P NMR spectra are reversibly interconverted, showing that no chemical reaction occurs in such a temperature range. The changes are only due to rapid dynamic phenomena in the wheel. The unambiguous assignments of the lines observed at 275 K to the parent $[ClP_2Mo_{12}]^{5-}$ or to other species

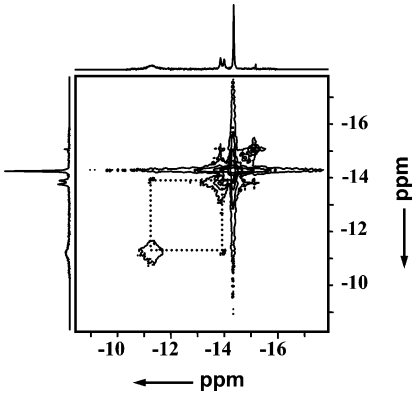

Figure 8. Contour plot of a two-dimensional COSY ^{31}P experiment for **1** at 275 K. The mixing time was 100 ms.

required further NMR experiments. The doublet at −13.80 ppm and the broad band at −11.15 ppm could correspond to two coupled inequivalent phosphorus nuclei of a single $\{P_2O_7\}$ group. The two lines are always in a 1:1 ratio, and the doublet would correspond to the first component of an AB coupling system in an asymmetrical pyrophosphate group. The coupling constant exhibits the usual value expected for such a system ($^2J_{P-O-P} = 16$ Hz). Finally, the asymmetric shape of the broad band (−11.15 ppm) would be due to the second unresolved component of the AB system. To confirm this assumption, a two-dimensional COSY ^{31}P NMR experiment was carried out (Figure 8) and clearly showed that the two lines at −13.80 and −11.15 ppm are correlated by two off-diagonal spots. They can therefore be definitely assigned to a single asymmetrical $\{P_2O_7\}$-containing species. The $^2J_{P-O-P}$ indirect coupling constant is strongly dependent on the angle P−O−P. Some examples of pyrophosphate embedded in polyoxometalate architectures give correlated values between the P−O−P angles and the corresponding coupling constant. In $[(P_2O_7)Mo_6O_{18}(OH_2)]^{4-}$, the P−O−P angle is 122.6°, corresponding to $^2J_{P-O-P} = 10.3$ Hz.[22] The opening of the P−O−P angle to 180°, observed in the cigar-shaped $[(P_2O_7)_2Mo_{30}O_{90}]^{8-}$ anion, increases significantly the $^2J_{P-O-P}$ constant to 36 Hz.[23] The 16 Hz value corresponds to that observed here for $[(H_2P_3)Mo_{10}]^{3-}$ (**3**) (see below), which exhibits a 130° P−O−P angle in the solid state. Accordingly, the mean angle value in the asymmetrical $\{P_2O_7\}$ group should be close to 130°, significantly lower than the observed P−O−P angle (150°) of the symmetrical $\{P_2O_7\}$ in $[Cl(P_2)Mo_{12}]^{5-}$ (**1**). Finally, both set of resonances δ_1 and ($\delta_2 - \delta_2$*) probably arise from a common $\{P_2Mo_{12}\}$ architecture, containing two strictly equivalent phosphorus nuclei (symmetrical conformation giving δ_1) or two inequivalent phosphorus (asymmetrical conformation giving $\delta_2 + \delta_2$*), respectively.

The influence of the halide ion concentration (Cl^-, Br^-, and I^-) on the distribution of the two main resonances was studied while the ionic strength was maintained constant at 2 M by varying the concentration of sodium nitrate and sodium chloride, $[NaNO_3] + [NaX] = 2.00$ mol·L^{-1}. The results graphically presented in Figure 9a clearly show the influence of the chloride concentration upon the distribution of the two sets of resonances. When the concentration of chloride ion is varied from 0.03 to 2.00 mol·L^{-1}, the relative intensity of δ_1 (attributed to a

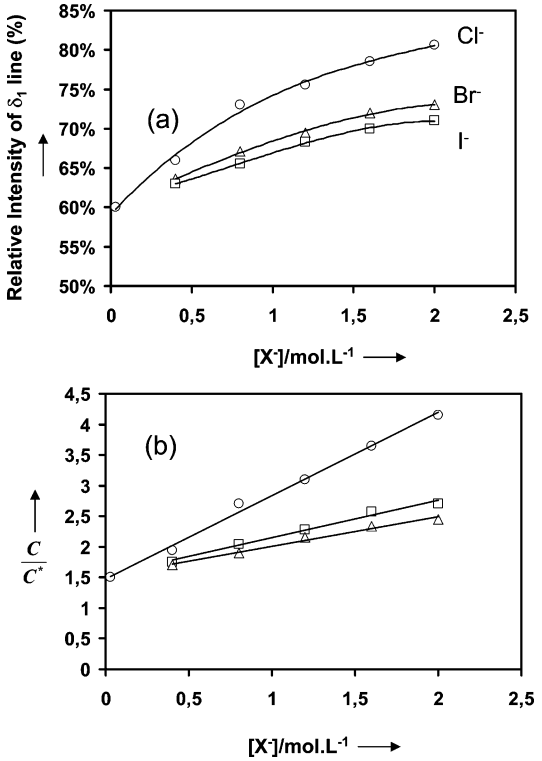

Figure 9. (a) Dependence of the δ_1 relative intensity versus the halide (Cl^-, Br^-, and I^-) concentration. (b) Linear behavior justifying the two successive eqs 5 and 6.

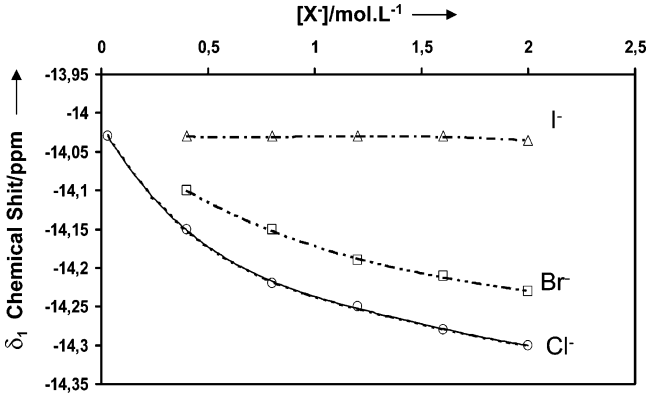

Figure 10. Influence of the nature of the halide X^- (X = Cl, Br, and I) upon the δ_1 chemical shift.

symmetric $\{P_2O_7\}$ group in a Mo_{12} ring) increased significantly from 60 to 80% (Figure 9a). Then, this line was attributed to a chloride-interacting species, probably structurally close to the ion parent **1** $[Cl(P_2)Mo_{12}]^{5-}$ (see Figure 3). This assumption is supported by the fact that only the δ_1 chemical shift is sensitive to the concentration of Cl^- (Figure 10), while the other δ_2, δ_2* resonances and that of the $[HP(P_2)Mo_{12}]^{6-}$ impurity remain quite constant. Then, the chloride ion interacts with the symmetrical $[(P_2)Mo_{12}]^{4-}$ hemicycle (through H-bonding) to form a labile ion-pairing complex $[Cl(P_2)Mo_{12}]^{5-}$. The chloride ion exchange is fast (Scheme 1), occurring statistically at both sides of the aperture of the hemicycle; it is characterized by the δ_1 single line. Removal of the chloride ion from the aperture of the cycle provokes a change in the conformation of the molecule, noted $[(PP^*)Mo_{12}]^{4-}$ and characterized by an asymmetrical $\{P_2O_7\}$ group within the cavity. The δ_2 resolved doublet would correspond to the $\{P_2O_7\}$ part strongly anchored within the ring

(22) Kortz, U. *Inorg. Chem.* **2000**, *39*, 625.
(23) Kortz, U. *Inorg. Chem.* **2000**, *39*, 623.

Scheme 1

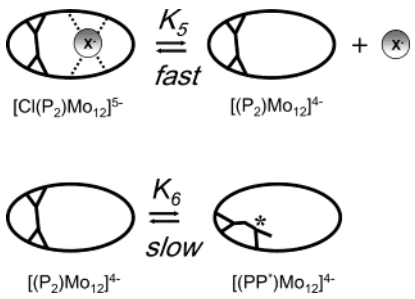

via double-bonded oxygen atoms. The δ_2* broad signal would correspond to the other parts of the $\{P_2O_7\}$ group, showing the possibility for the phosphate to hop from each side of the inner wall of the cavity (see Figure 11). The wriggling motion is temperature-dependent, giving a single emerging resonance at 305 K. In fact, at high temperature, the $\{P_2O_7\}$ group quickly hops in the cavity, making the two phosphorus nearly equivalent on the NMR time scale. A simple model can be proposed for the $[(PP^*)Mo_{12}]^{4-}$ anion which results from the 90° rotation of the $\{P_2O_7\}$ group. Finally, the ^{31}P NMR of **1** in aqueous solution can be explained by the presence of two main species, differing by their ring conformation, one giving a symmetrical "blocked" $\{P_2O_7\}$ guest (noted $[P_2Mo_{12}]^{4-}$) while the other one (noted $[PP^*Mo_{12}]^{4-}$) permits a wriggling motion of the asymmetrical $\{P_2O_7\}$ in the wheel. As the ratio between the two forms can be tuned by the chloride ion, two successive eqs, 5 and 6, are proposed.

$$[Cl(P_2)Mo_{12}]^{5-} \rightleftharpoons Cl^- + [(P_2)Mo_{12}]^{4-} \quad (5)$$

$$[(P_2)Mo_{12}]^{4-} \rightleftharpoons [(PP^*)Mo_{12}]^{4-} \quad (6)$$

The dynamic of eq 5 was deduced to be fast on the NMR time scale, and thus the weight of the δ_1 line is related to the concentration C corresponding to the sum of the concentration of the two species $[ClP_2Mo_{12}]^{5-}$ and $[P_2Mo_{12}]^{4-}$. The concentration C* of the $[PP^*Mo_{12}]^{4-}$ anion was directly calculated from the intensity of the δ_2 and δ_2* lines. Finally, the convenient linear eq 7, including K_5, K_6, the concentration of the chloride ion $[Cl^-]$, C, and C*, was established, where K_5 and K_6 are the constants of eqs 5 and 6, respectively. The linear plot of C/C^* versus $[Cl^-]$, shown in Figure 9b, is in agreement with the postulated equations and the ^{31}P NMR attributions. According to eq 7, the equilibrium constants $K_6 = 0.60$ and $K_5 = 1.09$ were found.

$$\frac{C}{C^*} = \frac{1}{K_6} + \frac{1}{K_5 K_6}[Cl^-] \quad (7)$$

The influence of the nature of the halides ($X^- = Cl^-$, Br^-, and I^-) upon the successive eqs 5 and 6 was studied, and the results are graphically shown in Figure 9 and summarized in Table 2. In agreement with eq 6, the constant K_6 does not vary significantly with the nature of the halide ($K_6 = 0.63 \pm 0.03$). In contrast, the constant K_5 is significantly increased in the order $I^- > Br^- > Cl^-$, meaning that the stability of the ion-pairing complex $[X(P_2)Mo_{12}]^{5-}$ is increased in the order $Cl^- > Br^- > I^-$.

$[(H_2P_3O_{10})Mo_{10}S_{10}O_{10}(OH)_{10}]^{3-}$ (3). The ^{31}P NMR spectrum of the triphosphate anion in aqueous solution, shown in Figure 12, presents two signals consisting of a doublet at −17.52 ppm and a triplet at −24.61 ppm with an 2:1 intensity ratio ($^2J_{P-O-P}$ = 16 Hz). The spectrum of **3** is not temperature-dependent, confirming the absence of dynamic in $[(H_2P_3)Mo_{10}]^{3-}$. The central $\{P_3O_{10}\}$ group is strongly blocked inside the ring through covalent interactions. In such a situation, the central guest has no possibility for changing its conformation through a concerted hopping in the cavity.

Conclusion

Polyphosphate ions easily react with cyclic oxothiomolybdic backbone, allowing the formation of encapsulated substrates. These compounds are quantitatively prepared in aqueous medium. Their molecular structure, established in the solid state, exemplified the adaptability and the potentialities of this class of compounds: different substrates can be incorporated, differing by the nature of the host−guest interactions, either through H-bonding or through iono-covalent interactions. A ^{31}P NMR study (variable temperature and 2D COSY experiment) reveals that supramolecular interactions between halide X^- (X = Cl, Br, or I) and the ring are maintained even in solution for giving the labile anion $X^- \subset [P_2Mo_{12}]^{5-}$. In addition, the possibility to remove selectively the halide ions for a monophosphate $[HPO_4]^{2-}$ ion in the $[P_2Mo_{12}]^{4-}$ compound is a promising route for the synthesis of a more sophisticated multiring assembly such as a dumbbell-shape compound with the use of specific polytopic ligand as polyphosphonate or polycarboxylate.

Experimental Section

Synthesis. All reagents were used as purchased without further purification. The cyclic precursor was prepared by the synthetic procedure described in ref 12. The previous characterization of this crude precursor led to the composition $K_2I_2[Mo_{10}S_{10}O_{10}(OH)_{10}(H_2O)_5]\cdot 15H_2O\cdot\epsilon Me_4NCl$ (noted $K_2I_2Mo_{10}$).

$K_5[Cl(P_2O_7)Mo_{12}S_{12}O_{12}(OH)_{12}(H_2O)_4]\cdot 22H_2O$ (1). $K_2I_2Mo_{10}$ (3 g, 1.30 mmol) was dissolved in 120 mL of distilled water under moderate heating (35−40 °C). Then, $Na_4P_2O_7\cdot 10H_2O$ (0.47 g, 1.04 mmol) was added. After 15 min, the solution was cooled to ambient temperature, and potassium chloride (18 g, 241 mmol) was added. The turbid solution was filtered until clear. The resultant filtrate was left standing at ambient temperature for crystallization. After 2 days, orange crystalline needles were isolated (1.60 g, yield 52%). Elemental analysis (%), calcd (found): K, 6.96 (6.98); Cl, 1.26 (1.32); P, 2.21 (2.15); Mo, 41.06 (42.10). IR $\bar{\nu}$/cm^{-1}: 1128 (m), 1053 (m), 1032 (sh), 950 (s), 907 (s), 693 (vw), 572 (m), 510 (s), 408 (w), 334 (w).

$K_6[(HPO_4)(P_2O_7)Mo_{12}S_{12}O_{12}(OH)_{12}(H_2O)_2]\cdot 23H_2O$ (2). $K_2I_2Mo_{10}$ (3 g, 1.30 mmol) was dissolved in 120 mL of distilled water under moderate heating (35−40 °C). Then, $Na_4P_2O_7\cdot 10H_2O$ (0.47 g, 1.04 mmol) was added. After 15 min, the solution was cooled at ambient temperature, and potassium chloride (18 g; 241 mmol) was added. The turbid solution was filtered until clear. Then KH_2PO_4 (0.18 g, 1.32 mmol) was added. After about 2 h, an orange crystalline precipitate was isolated (2.60 g, yield 85%). Elemental analysis (%), calcd (found): K, 8.34 (8.62); P, 3.30 (3.25); Mo, 40.94 (41.02). IR $\bar{\nu}$/cm^{-1}: 1152 (sh), 1133 (w), 1056 (m), 941 (s), 916 (s), 714 (w), 577 (w), 500 (m), 423 (sh), 341 (w). ^{31}P NMR, D_2O-H_2O solution about 0.03 mol·L^{-1} in (**2**): −13.9 ppm (2P), −1.8 ppm (1P).

Single crystals of (**2**) were obtained by recrystallization of the crude powder (about 0.4 g) in 20 mL of 0.5 mol·L^{-1} KCl aqueous solution. After 1 day, orange diamond-shaped crystals were obtained, suitable for single-crystal X-ray diffraction.

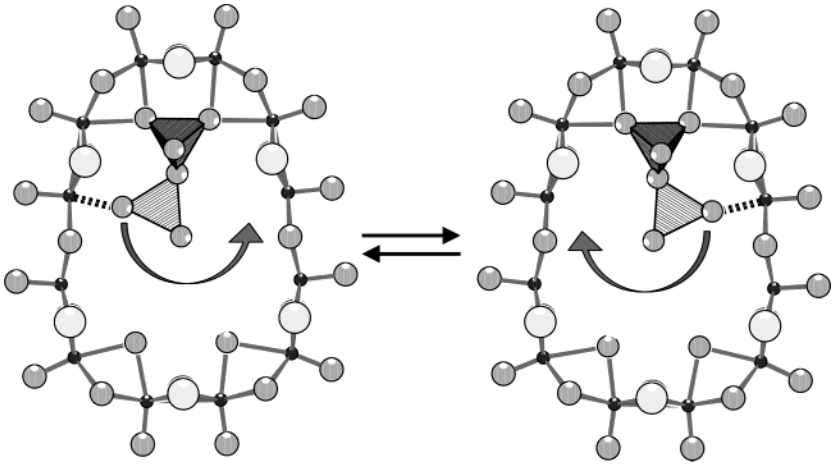

Figure 11. Postulated conformation for the "wriggling" asymmetrical pyrophosphate group in a Mo_{12} architecture with anchored and wheeling (schematized by arrows) $\{PO_4\}$ moieties.

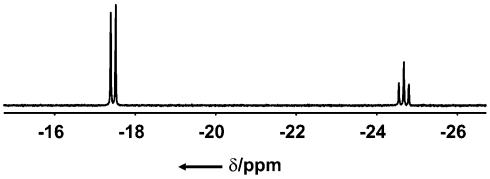

Figure 12. ^{31}P NMR spectrum of $[(H_2P_3O_{10})Mo_{10}S_{10}O_{10}(OH)_{10}]^{3-}$ (**3**).

Table 2. Equilibrium Constants K_5 and K_6 at $T = 275K$

X^-	K_5	K_6
Cl^-	1.09	0.60
Br^-	2.51	0.65
I^-	3.17	0.65

$Rb_3[(H_2P_3O_{10})Mo_{10}S_{10}O_{10}(OH)_{10}]\cdot 17.5H_2O$ (3). $K_2I_2Mo_{10}$ (3 g, 1.30 mmol) was dissolved in 120 mL of distilled water under moderate heating (50 °C). Then, $Na_5P_3O_{10}$ (0.47 g, 1.30 mmol) was added. After 15 min, RbCl (2 g, 16.5 mmol) was added to the warm solution. The rubidium salt of **3** slowly precipitated from the hot solution (50 °C). Orange rubidium salt was washed with ethanol, and then dried with diethyl ether (2.1 g; yield 70%). Elemental analysis (%), calcd (found): Rb, 10.48 (10.65); P, 3.82 (3.94); Mo, 39.46 (37.65); S, 13.15 (12.95). IR $\bar{\nu}/cm^{-1}$: 1235 (m), 1162 (sh), 1122 (m), 1048 (w), 1034 (w), 1005 (w), 940 (s), 736 (w), 709 (w), 604 (vw), 563 (m), 507 (m), 413 (w), 314 (m). ^{31}P NMR, D_2O-H_2O solution about 0.01 mol·L-1 in (**3**): −17.52 ppm (doublet, 2P); −24.61 ppm (triplet, 1P).

Single crystals of (**3**) were obtained by recrystallization of the crude powder (about 0.1 g) in 20 mL of water. After one week, parallelepipedic orange crystals were obtained, suitable for single-crystal X-ray diffraction.

Elemental analysis was performed by the Service Central d'Analyses du CNRS. The water content was determined by thermal gravimetric analysis (TGA experiments) with a TGA7-Perkin-Elmer apparatus.

Infrared spectra were recorded on an IRFT Magna 550 Nicolet spectrophotometer using the technique of pressed KBr pellets.

^{31}P NMR spectra were recorded at the nominal frequency of 121.5 MHz (Bruker AC 300 apparatus). Spectra were referenced to external 85% H_3PO_4 in 5 mm tubes.

X-ray Crystallography. Intensity data collection was carried out at room temperature with a Siemens SMART-CCD area detector system equipped with a normal-focus molybdenum-target X-ray tube (λ = 0.71073 Å). Crystals of **1** and **2** were mounted in glass tube because they rapidly lose water of crystallization, leading to an amorphous solid. An empirical absorption correction was applied (SADABS program[24] based on Blessing's method[25]). The structures were solved by direct methods and refined by the full-matrix least-squares procedure (SHELX-TL package).[26] Relevant crystal data for compounds **1**, **2**, and **3** are summarized in Table 1. Heavier atoms for each structure were initially located by direct methods. The remaining non-hydrogen atoms were located from Fourier differences and were refined with anisotropic thermal parameters.

$K_5[Cl(P_2)Mo_{12}]\cdot 22H_2O$ (1). The inner pyrophosphate and chloride ion adopt two enantiomeric conformations related by an inversion center located at the center of the Mo_{12} ring. The resulting atoms P1, P2, O17, O18, O19, and Cl were refined with occupancy factor of 1/2. All the potassium cations were found to be disordered and refined with a statistical occupancy factor of 1/2.

$K_6[HP(P_2)Mo_{12}]\cdot 23H_2O$ (2). The inner monophosphate and pyrophosphate adopt two enantiomeric arrangement related by a mirror plane containing the 12 Mo atoms of the ring. As a result, the two enantiomeric forms appear statistically distributed over the same crystallographic site, leading to a 1/2 occupancy factor for the phosphorus atoms P1, P2, and P3 and the P-bounded 027, O28, 029, O30, O31, and 024 oxygen atoms. All the potassium cations were found to be disordered and refined with a statistical occupancy factor of 1/2, excepted for the K7 atom (S.O.F of 0.25).

$Rb_3[H_2(P_3)Mo_{10}]\cdot 17.5\ H_2O$ (3). The central P2 phosphorus atom of the linear $\{P_3O_{10}\}$ group in the Mo_{10} ring was found to be disordered over two positions labeled P2A and P2B, refined with statistically occupancy factors of 2/3 and 1/3, respectively. The corresponding P2-bounded O16 and O17 oxygen atoms were refined with adequate statistical occupancy factors of 2/3 and 1/3 when labeled A and B, respectively. One rubidium atom was split over the two neighboring Rb2 and Rb3 sites, with statistical occupancy factors of 2/3 and 1/3, respectively, while the remaining 0.33 rubidium atom could be distributed over the Rb4 and Rb5 sites with statistical occupancy factors of 0.24 and 0.19, respectively.

Supporting Information Available: Further details on the crystal structures of **1**, **2**, and **3** (CIF). This material is available free of charge via the Internet at http://pubs.acs.org.

JA048746A

(24) Sheldrick, G. M. *SADABS*; Program for scaling and correction of area detector data; University of Göttingen: Göttingen, Germany, 1997.
(25) Blessing, R. *Acta Crystallogr*. **1995**, *A51*, 33.
(26) (a) Sheldrick, G. M. *Acta Crystallogr*. **1990**, *A46*, 467. (b) Sheldrick, G. M. *SHELX-TL*, version 5.03; Software Package for the Crystal Structure Determination; Siemens Analytical X-ray Instrument Division: Madison, WI, 1994.